Journal of Biomaterials Applications

Synthesis and characterization of Fe3O4@GT/PVA nanocomposite for hydroxychloroquine sulfate (HCQ) delivery

Journal:	*Journal of Biomaterials Applications*
Manuscript ID	Draft
Manuscript Type:	Original Manuscript
Keywords:	PVA, GT, HCQ, drug release, nanocomposite, hydrogel
Abstract:	Recent studies have shown the potential of hydroxychloroquine (HCQ) as a pharmaceutical agent to the treatment of a variety of cancers such as lung, melanoma, breast, pancreatic, and colon cancers. HCQ has been proposed to cure viral diseases such as Covid-19 disease. nowadays; Many studies for drug delivery of HCQ to the target site have been Developed through nanocomposite system. In this study, Fe3O4@PVA/GT nanocomposite has been synthesized for controlling HCQ release at pH 7.4. The influence of different factors were studied on the swelling and releasing rate such as the ratio of PVA to GT, the amount of Fe3O4 and the amount of crosslinking agent (citric acid), by the Tguchi method with 4 factors at 5 levels. The obtained results showed that increasing the amount of GT to PVA decreased the drug release rate. In improving the swelling, even a small amount of citric acid is effective, but its high amount reduces the swelling rate. After 18 hours, sample with PVA / GT ratio 100:0 (%wt), 2% CA (%wt) and 4% Fe3O4 (%wt) had the highest cumulative drug release (80.28 %) and sample with PVA / GT 85:15 (%wt), 4% CA (%wt) and 3% Fe3O4 (%wt) had the lowest cumulative drug release (39.28%).

Synthesis and characterization of Fe_3O_4@GT/PVA nanocomposite for hydroxychloroquine sulfate (HCQ) delivery

Abstract:

Recent studies have shown the potential of hydroxychloroquine (HCQ) as a pharmaceutical agent to the treatment of a variety of cancers such as lung, melanoma, breast, pancreatic, and colon cancers. HCQ has been proposed to cure viral diseases such as Covid-19 disease. nowadays; Many studies for drug delivery of HCQ to the target site have been Developed through nanocomposite system. In this study, Fe_3O_4@PVA/GT nanocomposite has been synthesized for controlling HCQ release at pH 7.4. The influence of different factors were studied on the swelling and releasing rate such as the ratio of PVA to GT, the amount of Fe_3O_4 and the amount of crosslinking agent (citric acid), by the Tguchi method with 4 factors at 5 levels. The obtained results showed that increasing the amount of GT to PVA decreased the drug release rate. In improving the swelling, even a small amount of citric acid is effective, but its high amount reduces the swelling rate. After 18 hours, sample with PVA / GT ratio 100:0 (%wt), 2% CA (%wt) and 4% Fe_3O_4 (%wt) had the highest cumulative drug release (80.28 %) and sample with PVA / GT 85:15 (%wt), 4% CA (%wt) and 3% Fe_3O_4 (%wt) had the lowest cumulative drug release (39.28%).

Keywords: PVA, GT, HCQ, hydrogel, drug release, CA, nanocomposite

1. Introduction:

Conventinal drug delivery systems (DDSs), like pills and capsules, a slight dose of the drug reaches the target site. The healthy tissues might also be affected due to passing through the gastrointestinal tract or circulatory system [1, 2]; but Targeted drug delivery leads to the accumulation of drugs in a specific body area. The main advantage of using targeted drug delivery is to increase the therapeutic effects of the drug without inducing side effects on healthy tissues and cells more [3,4]. The drugs can be delivered to the target tissues by magnetic field, light, and heat. Among these, magnetic nanoparticles (MNPs) are widely used as targeting drug carriers due to their high magnetic properties, fewer expences, and easy production [5,6]. However, MNPs are not used alone and are utilized in combination with other materials; because the bare MNPs often have poor stability and dispersity [7,8].

Magnetic nanocomposites are a new area of research on superparamagnetic nanomaterials for the targeted drug delivery using an external field. Supermagnetic Fe_3O_4 NPs can be an important component of magnetic nanocomposites due to properties such as targeted transfer, local hyperthermia treatment, and contrast enhancement for magnetic resonance imaging [9]. Hydrogels can be used as a second component of these nanocomposites, which can trap the drug in their network structure and release the drug due to the high water absorption [10,11].

Nowadays, carboxymethylcellulose (CMC)-polyvinyl alcohol (PVA)-Fe_3O_4 magnetic nanocomposites have been developed for long-term drug release. Citric acid, maleic anhydride and glutaraldehyde can be used to make crosslink between network structure of these hydrogels. The presence of -COOH groups in these hydrogels is useful because they are usually ionized at physiological pH and are more desirable to deliver the drug to the target. The presence of OH groups in PVA also increases the flexibility of the hydrogel film. In addition, crosslink agents may hold drug molecules in the hydrogel matrix by hydrogen bonding and electrostatic

interactions bteween –OH and -COOH [12,13]. Among Natural polymers, Tragacanth gum (GT) has been attracted much attention due to non-toxicity, biodegradability, biocompatibility, cost-effectiveness and easy access, as well as wound healing, and suitable antimicrobial properties[14]. This valuable natural substance obtained from Middle East farms can be a good alternative to industrial hydrogels such as PVA. It is sensitive to pH and therefore can be used as a smart drug carrier sensitive to physiological pH [15,16].

In this project, a novel PVA /GT/Fe_3O_4 nanocomposite has been developed and Hydroxychloroquine sulfate (HCQ) is used as a model to evaluate the drug release rate from PVA /GT/Fe_3O_4 nanocomposite. HCQ known as a drug to treat certain types of malaria [17]. Treating rheumatoid arthritis, lupus erythematosus, and Porphyria cutanea tarda are other uses. Also, it has been used to treat lung and intestine cancer. HCQ can act as a promising chemical sensitizer and immunomodulator for lung cancer chemotherapy. To treat some cancers, HCQ is mainly taken orally, which causes much damage to the cells. For lung cancer, drug can be directly delivered into the lungs by inhalation and in powder form to reach higher doses of the drug to the lungs and reduce the negative effects of the drug on other areas [1,2]. HCQ, with the outbreak of coronavirus (Covid-19), is used as an experimental drug for this disease. HCQ affects the entry of the corona virus in cells and raises the pH of the endosome. In addition, the process of endocytosis and the phenomenon of virus replication are eliminated. Therefore, HCQ plays an important role in viral infections[19].

According to researches; transmission of this drug to cancerous tissues by drug carriers can help improve the disease process; Because the drug reaches the target site and the drug release rate can be controlled[18].

Because HCQ is soluble in water, liposomes (such as PEG), polymeric NPs (such as PLGA), and Niosomes (such as Pluronic F-127) can be used for delivery systems of this drug [20]. Nano-carriers based on Fe_3O_4 have also been used as a suitable carrier of this drug (for example Fe_3O_4@SiO_2@GLYMO@pectin). Due to their good magnetic properties, they can deliver the drug to the desired location with an external magnetic field [9].

.

In this project, hydrogel of poly vinyl alcohol (PVA) and tragacanth gum (TG) has been used for the targeted drug delivery system. Citric acid as a crosslinking agent is more preferred to maleic anhydride and glutaraldehyde due to its non-toxicity.

Finally, using taguchi method, parameters such as the ratio of PVA to GT, the amount of citric acid, and the amount of iron oxide in the HCQ release rate are examined; then, the sample with the most drug release will be selected as the optimal sample for PVA / GT / Fe_3O_4 magnetic hydrogel in the short term. Taguchi is one of the methods for optimizing experiments. This method uses orthogonal arrays (OA) to reduce the number of experiments [22]. In summary, the purpose of the Taguchi method is to be able to observe and identify output changes by making changes to process input variables and analyzing variance.

2. Materials and methods

2.1 Materials:

Hydroxychloroquine sulfate (Figure 1) was prepared from Amin Pharmaceutical Company (Iran), tragacanth gum (GT, MW=50000-100000) (Iran) was obtained from Iranian farms, and polyvinyl alcohol (PVA, MW: 10000-30000), $FeSO_4.7H_2O$, $FeCl_3.6H_2O$, citric acid (CA), NH_4OH and Buffer pill containing KCl, NaCl, Na_2HPO_4 and K_2HPO_4 were prepared from Sigma Aldrich.

Fig. 1.

2.2 Synthesis of Fe_3O_4:

The co-precipitation method was used to synthesize Fe_3O_4 nanoparticles [23]. First, 1 gram of $FeSO_4 \cdot 7H_2O$ and 1.62 gram of $FeCl_3.6H_2O$ was dissolved in 40 ml of distilled water and stirred 1h. Then, ammonium hydroxide (NH_4OH, 0.5 M) was added dropwise to the solution and stirred for 1h (pH=11). As much as 2% w/w citric acid as a coating agent was added to the obtained solution for modification of Fe_3O_4 nanoparticles. The obtained Fe_3O_4 nanoparticles was separated by magnet and washed several times by the distilled water. Finally, the sediment was placed in an oven at 40 °C for 24 hours to be dried completely. SEM, FTIR, and VSM were used to characterize the structure and properties of the obtained nanocomposite.

2.3 Synthesis of Fe_3O_4@PVA/GT hydrogel:

Different proportions of PVA (0.8-1g) and GT (0-0.2g) were stirred in 20 ml distilled water using a mechanical stirrer; the solution was heated to 80 °C to form a gel. After 5 minutes, CA (0.01-0.05g) was added to it. Finally, the Fe_3O_4 nanoparticles (0.01-0.05g) were added and then stirred until the nanoparticles were completely dispersed.

At the end, the solution was poured into the petri dish and put in the oven at 40 °C to dry [12]. The produced film was placed in the oven and heated to 130 °C for a specified time (1-5 min) to

initiate crosslinking reaction. Figure 2 shows a schematic representation for synthesis of Fe_3O_4@PVA/GT hydrogel.

Fig. 2

2.4 Experimental design

The number of samples for the experiment was determined using Taguchi method with 4 factors and 5 levels (Table 1). The effect of parameters on the drug releasing including PVA:GT ratio, CA crosslinker wt.%, Fe_3O_4 wt.%, and crosslinking time (min) were investigated.

Table 1

Here, L25 (5^6) ANOVA was selected, which shows 25 experiments with 5 levels, 4 factors orthogonal array (Table 2).

Table 2.

2.4 Swelling study:

The quality of swelling can examine transverse bonds and chemical interactions between nanoparticles and hydrogels. 0.2 g of hydrogel film was placed in a dialysis bag and put in 20 ml of PBS buffer and the swollen film sample was removed from the buffer at different intervals (0.5, 1, 3, 6, 12, and 18h). Their surface water was dried with a paper towel and weighed. The swelling ratio was determined using the following equation.

$$\text{Swelling ratio} = \frac{(W_t - W_d)}{W_d} \qquad (1)$$

Where, W_d is the weight of the dried gel before swelling and W_t is the weight of the swollen gel at time t.

2.5 Drug loading and release study

1 g of the film was dissolved in 10 ml distilled water to form a hydrogel. 0.02 gr of HCQ (table 1) was added to it. The hydrogel was stirred for 12 hour to load the HCQ in the hydrogel network and was dried in petri dishes at 40^0C for 18 hour.

The in-vitro release experiments were studied in buffered solution at pH=7.4 and temperature 37 ^{0}C. 1 gram of the prepared film was placed in beaker contain 10 ml PBS with pH=7.4 to slowly turn into a hydrogel. At certain time intervals, 2 ml PBS was removed from beaker to determine drug release by spectrophotometry. Drug release was calculated via spectrophotometry at λ_{max}=343 nm. After removing 2 ml of the sample for testing, the same amount of PBS was added to beaker to keep the volume constant.

2.6 Characterization:

X-Ray Diffraction (XRD) model Philips PW3040 was used to confirm the crystalline structure of Fe_3O_4 nanoparticles. Fourier Transmission Infrared Spectroscopy (FT-IR) model Lumex infralum FT-08 was utilized to investigate the coating of Fe_3O_4 particles and analysis of the nanocomposite. Vibrating Sample Magnetometer (VSM) model 7404 made in Lake Shore Cryotronics Company was used for the measurement of magnetic properties. FE-SEM was performed with a ZEISS Sigma 300 scanning electron microscope operating at 15Kv to observe

surface morphology of nanocomposite. For investigating the release of HCQ from nanocomposite, Shimadzu brand UV-Vis model 1900i was selected. Minitab software was used for Taguchi design to optimize the number of experiments.

3. Results and discussion:

3.1 Coating of Fe_3O_4:

Many studies have been done to investigate the toxicity of MNPs. The results showed that they had significant toxicity on some tissues and cells. Prepared MNPs is coated citric acid to decrease toxicity and enhance stability. it is used as a coating agent due to it biocompatibility because the MNPs surface may be exposed to biological agent. The coating of MNPs inhibits agglomeration and oxidation and improves their dispersion in a suspension[7].

X-ray diffractograms (XRD) of the CA-coated MNPs are shown in figure 3. A series of peaks were observed at 2θ = 18.28, 30.19, 31.78, 35.71, 43.45, 53.55, and 63.32, which are in good accordance with the cubic phase of Fe_3O_4 (Reference code: JPCD-00-001-1111 and JPCD-00-002-1035). The peaks are sharp and intense confirming the formation of highly crystalline MNPs. The crystallite size of MNPs was calculated using Debye Scherer equation [7,8].

Fig. 3.

FT-IR of CA-coated and uncoated MNPs are compared in Figure 4. FTIR shows the presence of a functional group of coating agents on the particle surface of Fe_3O_4. For bare Fe_3O_4, the broad band spectrum at 3420.16 cm^{-1} is due to the stretching vibration of O-H groups on the surface of the Fe_3O_4 nanoparticles; some molecular water may be trapped in the crystalline structure of Fe_3O_4. As a result, the broad band of the peak may be due to the OH bands of water. Coating

MNPs raised the broad bond because of existence OH bands in citric acid. The C=O vibration of COOH group in CA at 1710.35 cm^{-1} shifts to lower wavenumber with higher intensity at 1619.13 cm^{-1} revealing the binding of a CA radical to surface of Fe_3O_4 MNPs by adsorption of carboxylate (citrate) ions. It can be attributed to the formation of an iron complex with C=O, which weakens the C=O bond.

The 1385.17 cm^{-1} and 1078 cm^{-1} peaks are due to the symmetric stretching of COO^- and C=O and OH groups. The strong absorption band in 568.52 cm^{-1} is related to the Fe-O stretching band [7,8].

Fig. 4.

Field dependent magnetization (M vs. H) plot at 300K (Fig 5.) show superparamagnetic behavior of coated MNPs without magnetic hysteresis. The maximum magnetization was 65 emu/g. These stable Fe_3O_4 nanoparticles with high magnetic response can be used for magnetic drug targeting. The amount of nanoparticles in the hydrogel plays a major role in the quality of its transmission by the magnetic field; its high amount makes the hydrogel more sensitive to the magnetic field. Measurement of zeta potential showed that the surface charge of nanoparticles at neutral pH was negative (24.6 mV).

Fig. 5.

SEM images of Fe_3O_4 MNPs are shown in figure 6, the surface of Fe_3O_4 nanoparticles are roughness and have high agglomeratin with asymmetrical shape. might be due to the magnetic

dipole moment interaction. The particle size is in the nanometer range. agglomeratin of nanoparticles is very undesirable because it disrupts their uniform dispersion in the hydrogel.

Fig. 6.

3.2 Swelling behavior Fe_3O_4@PVA/GT hydrogel:

Figure 7 showed the swelling results in pH=7.4

Fig. 7.

Design of experiments (DOE) is used for analyzing the swelling results. Figures 8 and 9 show the swelling average value of mean for 1 and 18 hours, at pH=7.4, respectively.

Fig. 8.

Fig. 9.

The increasing Fe_3O_4 nanoparticles strongly affects the swelling at pH= 7.4 (Fig.) due to the elasticity reduction of the nanocomposite. The film of hydrogel becomes more fragile by increasing Fe_3O_4. Fe_3O_4 content can adjust the swelling behavior and magnetization of the hydrogel; As a result, its amount is very important.

Increasing the amount of GT and Fe_3O_4 darkens the color of the hydrogel. Pure PVA swells quickly, but swelling slows down by additional GT. Perhaps the reason is in GT networks as it

takes longer to open GT cells and absorb water. The elasticity of GT is lower than PVA, so increasing it reduces the elasticity of the nanocomposite.

Cross-linking is required even in smaller amounts. Its absence causes the GT to separate from the PVA network. The small amount of CA increases water absorption [7]. Its high amount reduces water absorption and increases the fragility of hydrogels due to crosslinking. Extending the crosslinking time gives CA a greater chance to crosslink. Figure 10 shows that by increasing the reaction time, there will be a greater amount of the thermodynamically material of (a).

Fig. 10.

GT polysaccharide has many functional groups such as -COOH. Swelling increased due to the presence of an increased number of hydroxyl and ester functional groups introduced by cross linking the PVA/TG backbone with CA. The multiplicity of these groups not only increases the swelling due to the interaction of water with OH and COOH groups but also changes the interaction of the hydrogel with the HCQ [3,4].

3.3 Release behavior of Fe_3O_4@PVA/GT:

Figure 11 shows the results of drug release in pH 7.4. Values are expressed as a percentage of the original value.The S/N ratio equation is shown below. S/N is selected based on larger-the-better.

$$\frac{S}{N} = -10\lg\left(\frac{1}{n\sum_{i=1}^{n} y_i^2}\right) \qquad (2)$$

In this equation, n is the number of repetitions per test (n = 1), and y is the percentage of cumulative drug release.

Fig. 11.

Fig. 12.

Fig. 13.

It is clear that increasing the Fe_3O_4 has intensified the HCQ release due to the disruption of the network structure by solid particles (Fig. 13). A large amount of nanoparticles causes agglomeration in parts of the hydrogel and its weight balance can be disturbed (Fig. 15). Also, increasing the amount of GT reduces the drug release. As a result, these parameters can change the dosage of the HCQ. Increasing the amount of GT reduces the drug release. The presence of COOH functional groups in the GT networks is a factor for reducing the rate of drug release because of its more interaction with the drug.

The dosage of the HCQ depends on the patient's condition and the type of treatment [25-27]. Therefore, the type of hydrogel can be determined to release a certain amount of drugs. For example, sample 4 is used when a high dose is required and sample 17 is employed when the lowest dose is needed.

3.4 FTIR results of Fe_3O_4@GT/PVA

Figure 14 shows the FTIR of Fe_3O_4@PVA/GT nanocomposite. The broad band spectrum at 3300-3700 cm^{-1} related to OH stretching from the intermolecular and intramolecular hydrogen bonds of PVA and GT. The peak of the OH band widens with increasing GT, it is due to the formation of a hydrogen band between the GT and PVA chains. The absorption bands in 2967 cm^{-1} is for asymmetric stretching vibrations of methylene groups in PVA. The band at 1748 cm^{-1} can be attributed to carbonyl and C-O groups. The absorption bonds are absorbed at about 1470 cm^{-1} and 1280 cm^{-1} as related to CH_3 and CH_2 bending. absorption bands can be seen at 1140 cm^{-1} (C-O stretching) and 970 cm^{-1} and 830 cm^{-1} (C=C bending) of TG [28-30].

Fig. 14.

3.5 SEM results of Fe_3O_4@GT/PVA

Figure 15 shows the morphology of the Fe_3O_4@PVA/GT nanocomposite. In SEM images, the porosity on the surface of the hydrogel are well visible.In figure 15 (b) lumps can be caused by the presence of Fe_3O_4 in the hydrogel. These nanoparticles are well coated by hydrogels. However, nanoparticles are not well dispersed in the nanocomposite and have agglomerated in a certain area, which is very undesirable.In figure 15 (d) a crack-like structure is observed for nanocomposites, which is probably due to the prohibited movement of GT clusters in the cavities of the PVA network[28-30].

Fig. 15.

3.6 Kinetic modeling

The drug release kinetics of HCQ for the sample with the highest release (sample 4) and the minimum release (sample 17) were investigated by fitting the zero-order via Higuchi and Hixon-Crowell models to determine the best kinetic model. The kinetic equations are specified below. The maximum amount of R-squared (R^2) determines the best kinetic equation.

$C = k_0 t$ (3) zero order

$Q = k_H t^{\frac{1}{2}}$ (4) Higuchi

$Q_0^{\frac{1}{3}} - Q_t^{\frac{1}{3}} = k_{HC} t$ (5) Hixon-Crowell

In these equations, *k* is the constant value, *t* is release time, *C* is the concentration of drug release at time *t*, and *Q* is the amount of drug release at time *t* [15].

Table 3.

Clearly, the zero order kinetic equation is appropriate for the data. It can be observed from this equation that the drug release concentration has been continuous and slow over time.

The results of this study are compared with those of other studies as summarized in the following table.

Table 4.

4. Conclusion

In this project, Fe_3O_4@GT/PVA nanocomposite, magnetic and pH sensitive has been produced to carry the hydroxychloroquine drug. Hydroxychloroquine is one of the most effective drugs against some of cancers. For this nanocomposite, the ratio of PVA to GT, the amount of citric acid crosslinker, and Fe_3O_4 on the quality of swelling and drug release was investigated. The swelling of this nanocomposite was examined at neutral pH. The results showed that increasing the amount of Fe_3O_4 caused the fragility of dry nanocomposite and reduced swelling and increased drug release. The presence of citric acid is beneficial, but high amount of it reduce swelling. Adding GT to PVA reduces the rate of drug release.

Declaration of competing Interest

The authors declare that there are no competing financial interests.

Acknowledgments:

The authors would like to express their gratitude to Islamic Azad University, Najafabad, Iran.

References

1. Li Y, Cao F, Li M, et al. Hydroxychloroquine induced lung cancer suppression by enhancing chemo-sensitization and promoting the transition of M2-TAMs to M1-like macrophages. *J Exp Clin Cancer Res* 2018; 37: 259.
2. Manic G, Obrist F, Kroemer G, et al. Chloroquine and hydroxychloroquine for cancer therapy. *Mol Cell Oncol* 2014;1(1):29911.
3. Poorvashree J, Suneela D. Novel drug delivery of dual acting prodrugs of hydroxychloroquine with aryl acetic acid NSAIDs: Design, kinetics and pharmacological study. *Drug Deliv Transl Res* 2017;7(5):709-730.
4. Gadhave RV, Mahanwar PA, Gadekar PT. Effect of glutaraldehyde on thermal and mechanical properties of starch and polyvinyl alcohol blends. *Des Monomers Polym* 2019;22(1):164–170.

5. Goodarz Naseri M, Bin Saion E, Abbastabar Ahangar H, et al. Synthesis and characterization of manganese ferrite nanoparticles by thermal treatment method. *J Magn Magn Mater* 2011;323:1745-1749.

6. Wangm G, Ma Y, Zhang L, et al. Facile synthesis of manganese ferrite/graphene oxide nanocomposites for controlled targeted drug delivery. *J Magn Magn Mater* 2016 ;401:647–650.

7. Dheyab MA, Aziz AA, Jameel MS, et al. Simple rapid stabilization method through citric acid modification for magnetite nanoparticles. *Sci Rep* 2020;10:10793.

8. Wei Y, Han B, Hu X, et al. Synthesis of Fe_3O_4 Nanoparticles and their Magnetic Properties. *Procedia Eng* 2012;27:632-637.

9. Sadr MS, Heydarinasab A, Panahi HA, Javan RS. Production and characterization of biocompatible nano-carrier based on Fe_3O_4 for magnetically hydroxychloroquine drug delivery. *Polym Adv Technol* 2021;32:564–573.

10. Ponco A, Helmiyati H. Hydrogel of carboxymethyl cellulose and polyvinyl alcohol modified by CuNPs as antibacterial in wound dressing. *AIP Conference Proceedings* 2020;2242:040009.

11. Luo YL, Zhang XY, Fu JY, et al. Novel temperature and pH dual-sensitive PNIPAM/CMCS/MWCNT semi-IPN nanohybrid hydrogels: Synthesis, characterization, and DOX drug release. *Int J Polym Mater* 2017;66:398– 409.

12. Ghorpade VS, Dias RJ, Mali KK, Mulla SI, Citric acid crosslinked carboxymethylcellulose-polyvinyl alcohol hydrogel films for extended release of water soluble basic drugs. *J Drug Deliv Sci Technol* 2019;52:421-430.

13. Hoare TR, Kohane DS. Hydrogels in drug delivery: Progress and challenges. *Polymer* 2008;49:1993-2007.

14. Hosseini MS, Hemmati K, Ghaemy M. Synthesis of nanohydrogels based on tragacanth gum biopolymer and investigation of swelling and drug delivery. *Int J Biol Macromol* 2015;82:806-815.

15. Shafiee S, Abbastabar Ahangar H, Saffar A. Taguchi method optimization for synthesis of Fe_3O_4@ chitosan/Tragacanth Gum nanocomposite as a drug delivery system. *Carbohydrate Polymers* 2019;222:114982.

16. Niknia N, Kadkhodaee R, Eshtiaghi MN. Microbial Exopolysaccharides as Drug Carriers. *Polymers (Basel)* 2020;157:151-157.

17. Lei ZN, Wu ZX, Dong S, et al. Chloroquine and hydroxychloroquine in the treatment of malaria and repurposing in treating COVID-19. *Pharmacol Ther* 2020 Dec;216:107672.

18. Verbaanderd C, Maes H, Schaaf MB, et al. Repurposing Drugs in Oncology (ReDO)-chloroquine and hydroxychloroquine as anti-cancer agents. *Ecancermedicalscience* 2017;11:781.

19. Kavanagh O, Marie Healy A, Dayton F, et al. Inhaled hydroxychloroquine to improve efficacy and reduce harm in the treatment of COVID-19. *Med Hypotheses* 2020 ;143, 110110.

20. Stevens DM, Crist RM, Stern ST. Nanomedicine Reformulation of Chloroquine and Hydroxychloroquine. *Molecules* 2020;26(1):175.

21. Schroeder RL, Gerber JP. Chloroquine and hydroxychloroquine binding to melanin: Some possible consequences for pathologies. *Toxicology Reports* 2014;1:963-968.

22. Pouretedal HR, Damiri S, Zandi A. Study the operating conditions on agglomeration of RDX particles in anti-solvent crystallization by using statistical optimization. *Defence Technology* 2019;15:233-240.

23. Ajinkya N, Yu X, Kaithal Pet al. Magnetic Iron Oxide Nanoparticle (IONP) Synthesis to Applications: Present and Future. *Materials* 2020;13:4644.

24. Truong YB, Choi J, Mardel J, et al. Functional Cross-Linked Electrospun Polyvinyl Alcohol Membranes and Their Potential Applications. *Macromol Mater Eng* 2017; 302:1700024.

25. Al-Kofahi M, Jacobson P, Boulware DR, et al. Finding the dose for hydroxychloroquine prophylaxis for COVID-19; the desperate search for effectiveness. Clin Pharmacol Ther 2020;108(4) :766-769.

26. Badgujar K, Badgujar AB, Patil VP, Dhangar DV. Hydroxychloroquine for COVID-19: A review and a debate based on available clinical trials/case studies. *J drug deliv ther* 2020;10(3):304-11.

27. Borba MGS, Val FFA, Sampaio VS, et al. Effect of high vs low doses of chloroquine diphosphate as adjunctive therapy for patients hospitalized with severe acute respiratory syndrome coronavirus 2 (SARS-CoV-2) Infection: A Randomized Clinical Trial. *JAMA Netw pen* 2020;3(4):208857.

28. Kamoun EA, Kenawy ES, Chen X. A review on polymeric hydrogel membranes for wound dressing applications: PVA-based hydrogel dressings. *J Adv Res* 2017;8(3):217-233.

29. Ranjbar Mohammadi Bonab M, Prabhakaran M, Bahrami H, Ramakrishna S. Gum tragacanth/poly (l-lactic acid) nanofibrous scaffolds for application in regeneration of peripheral nerve damage. *Carbohydr Polym* 2015;140: 104-112.

30. Thambi T, Phan VHG, Lee DS. Stimuli-Sensitive Injectable Hydrogels Based on Polysaccharides and Their Biomedical Applications. *Macromol. Rapid Commun* 2016;37:1881–1896.

31. Zambuzi GC, Camargos CHM, Ferreira MP et al. Modulating the controlled release of hydroxychloroquine mobilized on pectin films through film-forming pH and incorporation of nanocellulose, *Carbohydr Polym* 2021; 2:100140.

32. Olejnik A, Goscianska J, On the importance of physicochemical parameters of copper and aminosilane functionalized mesoporous silica for hydroxychloroquine release. *Mater Sci Eng C* 2021;130: 112438.

33. Reddy SG. Controlled release studies of hydroxychloroquine sulphate (Hcq) drug-using biodegradable polymeric sodium alginate and lignosulphonic acid blends. *Rasayan Journal of Chemistry* 2021;*14(4):2209-2215*

34. Magne TM, Helal-Neto E, Correa LB et al. Rheumatoid arthritis treatment using hydroxychloroquine and methotrexate co-loaded nanomicelles: In vivo results. *Colloids Surf B* 2021; 206: 111952.

35. Armutcu C, Pişkin S. Evaluation of controlled hydroxychloroquine releasing performance from calcium-alginate beads. *Hittite J Sci Eng* 2021; 8(3): 255-263.

Figure captions

Fig. 1. Structure of HCQ [21]

Fig. 2. Synthesis of Fe_3O_4@GT/PVA nanocomposite

Fig. 3. XRD pattern of the CA-coated Fe_3O_4

Fig. 4. FTIR spectrum of CA-coated Fe_3O_4

Fig. 5. VSM results of CA-coated Fe_3O_4

Fig. 6. SEM images of nanoparticles

Fig. 7. Diagram of swelling at different hours in pH 7.4

Fig. 8. Mean at levels 1-5 for each parameter at pH=7.4 and 1 hour swelling

Fig. 9. Mean at levels 1-5 for each parameter at pH=7.4 and 18-hour swelling

Fig. 10. Reaction of CA and PVA at 130 °C [24]

Fig. 11. Diagram of HCQ release in pH=7.4

Fig. 12. Mean at levels 1-5 for each factor at pH 7.4

Fig. 13. SN ratio at levels 1-5 for each factor at pH 7.4

Fig. 14. FTIR spectra of a) sample 1 b) sample 3 c) sample 7 d) sample 11 e) sample 14 f) sample 20

Fig. 15. FE-SEM Image of a) sample 1, b) sample 7, c) sample 13 and d) sample 20

Table Captions:

Table 1. L25 Taguchi design (4 factors each at 5 levels) (* % ratio to total PVA and GT)

Table 2 The obtained experimental data from Taguchi method (* % ratio to total PVA and GT)

Table 3. Amount of R-squared (R^2) for sample 4 and 17

Table 4. HCQ delivery from different carriers

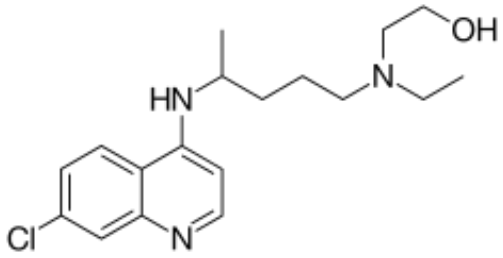

Fig. 1.

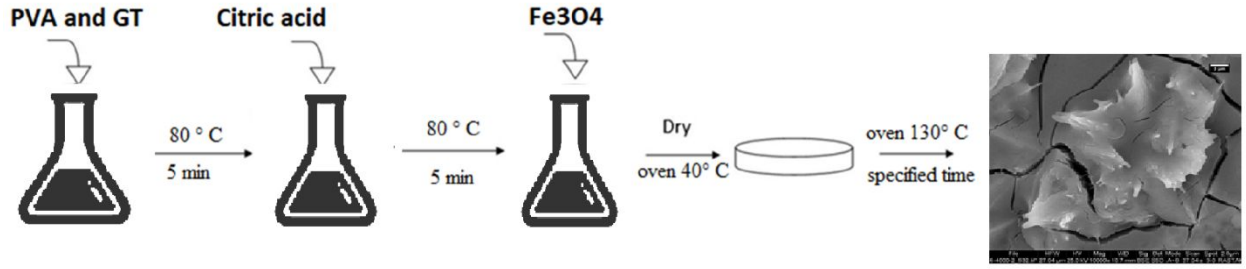

S

Fig. 2

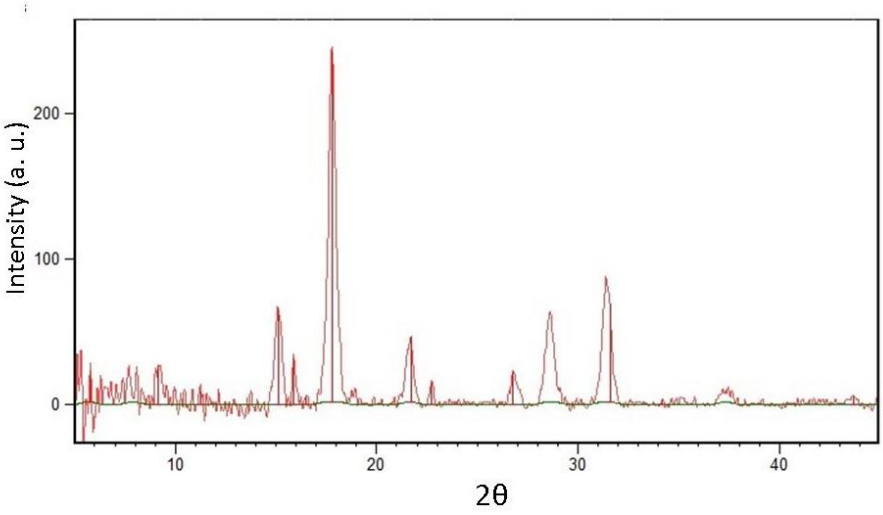

Fig. 3.

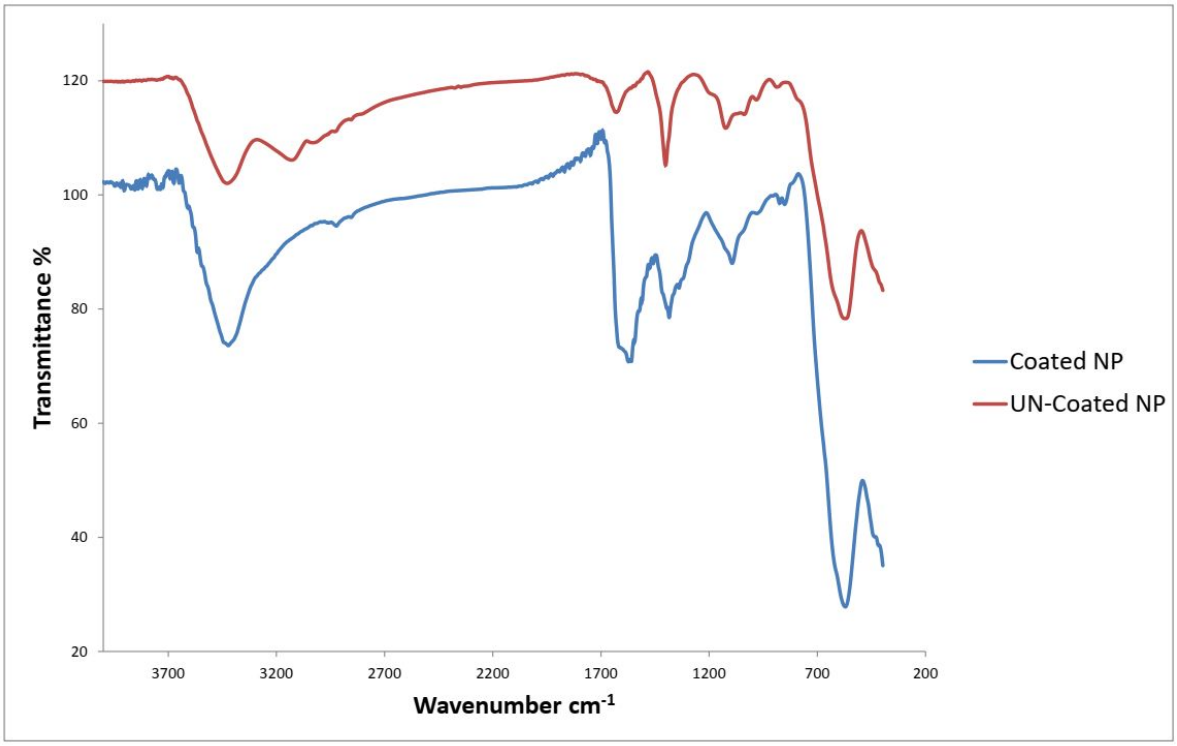
Transmittance %
120
100
80
60
40
20
3700
3200
2700
2200
1700
1200
700
200
Wavenumber cm-1
Coated NP
UN-Coated NP

Fig. 4.

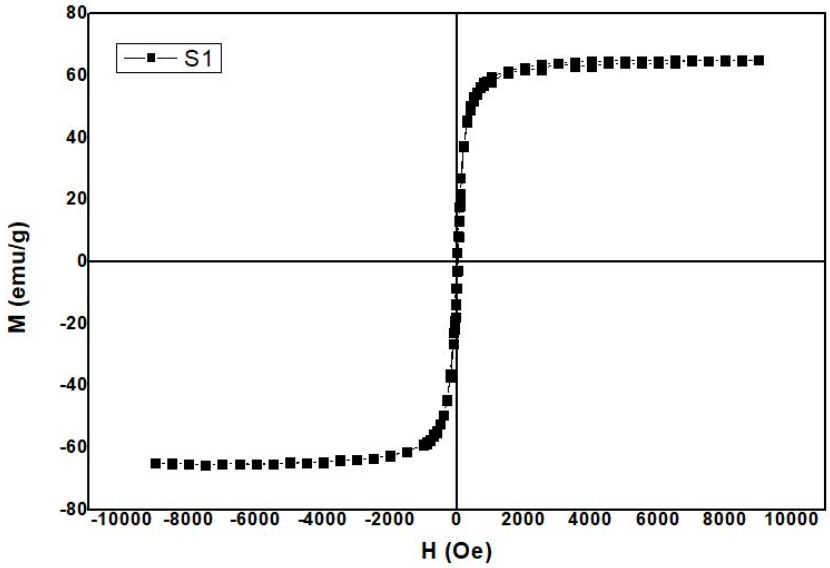
S1
M (emu/g)
80
60
40
20
0
-20
-40
-60
-80
-10000
-8000
-6000
-4000
-2000
0
2000
4000
6000
8000
10000
H (Oe)

Fig. 5.

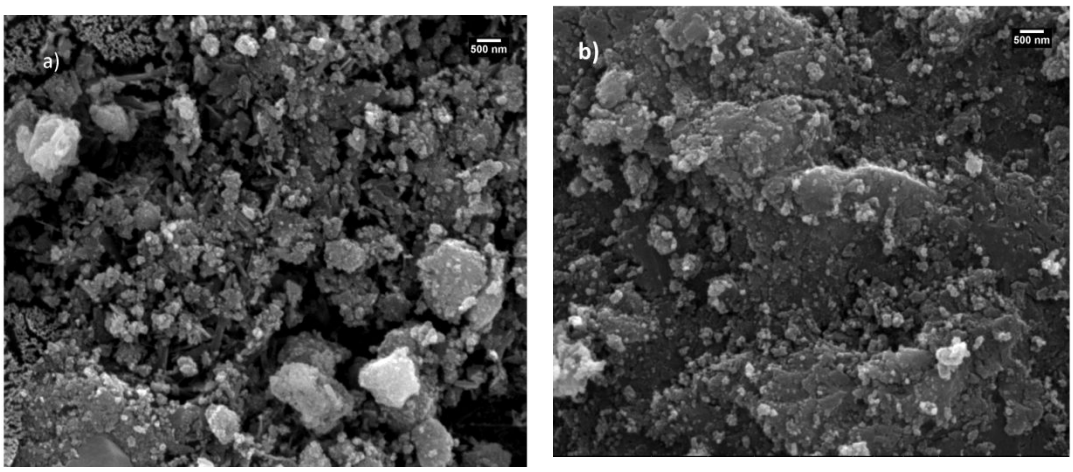
a)
500 nm
b)
500 nm

Fig. 6.

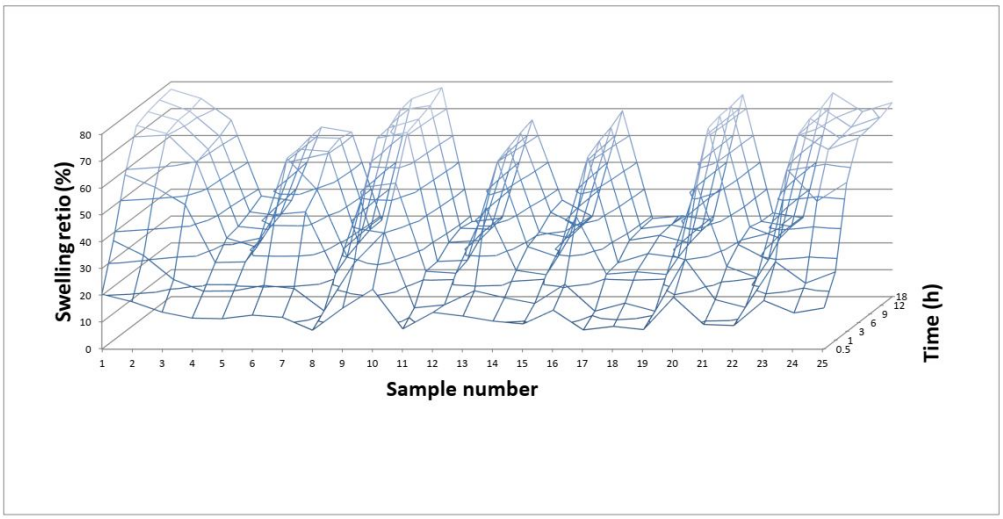
Swelling retio (%)
0
10
20
30
40
50
60
70
80
1 2 3 4 5 6 7 8 9 10 11 12 13 14 15 16 17 18 19 20 21 22 23 24 25
Sample number
0.5
1
3
6
9
12
18
Time (h)

Fig. 7.

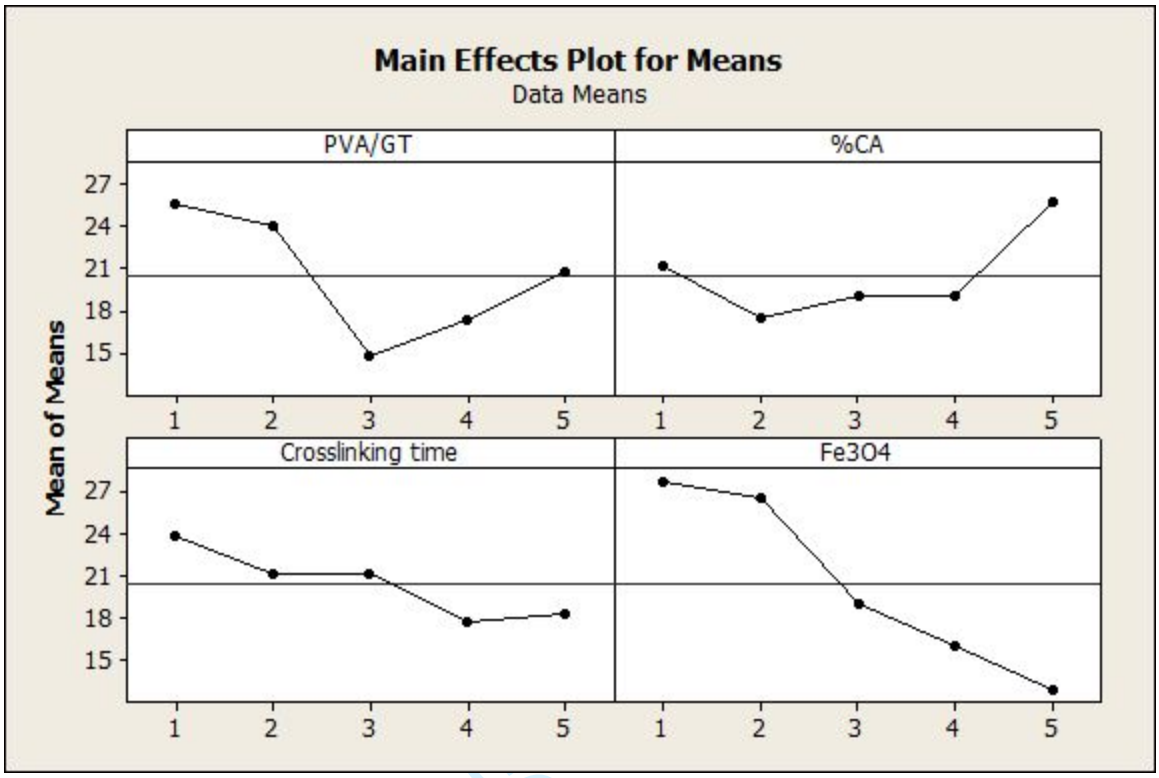

Fig. 8.

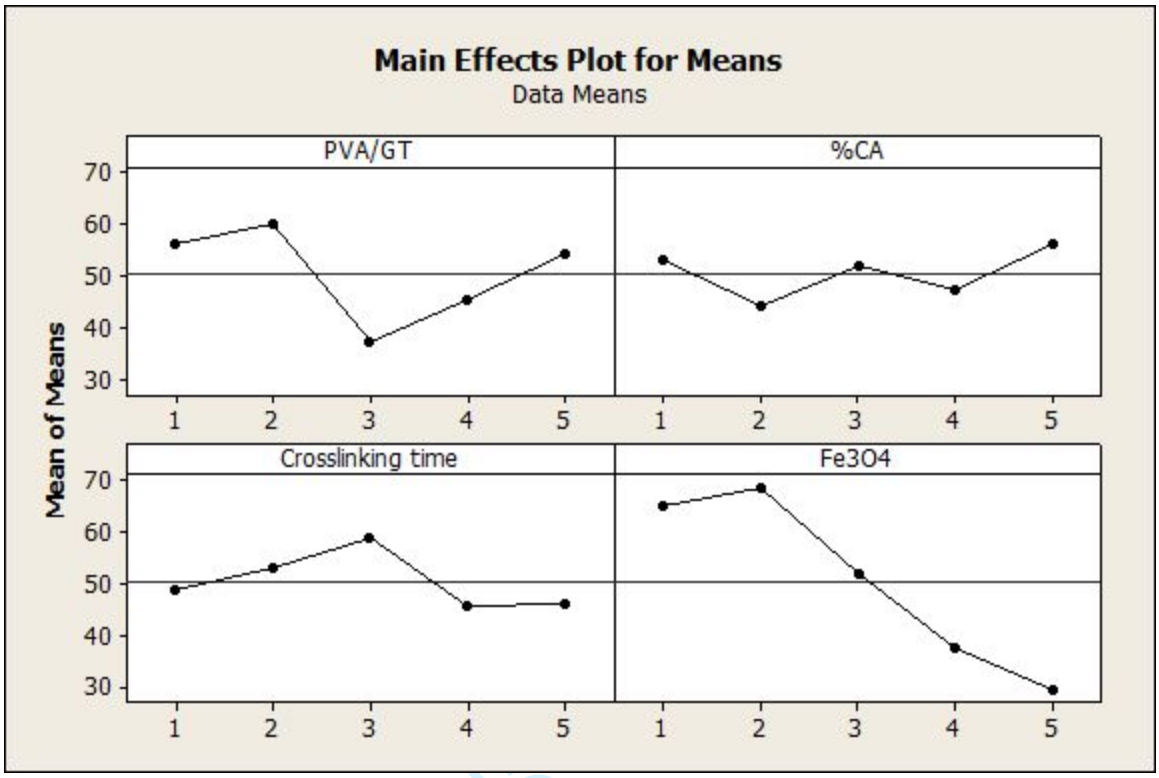
Main Effects Plot for Means
Data Means
PVA/GT
%CA
Crosslinking time
Fe3O4
Mean of Means
70
60
50
40
30
1
2
3
4
5

Fig. 9.

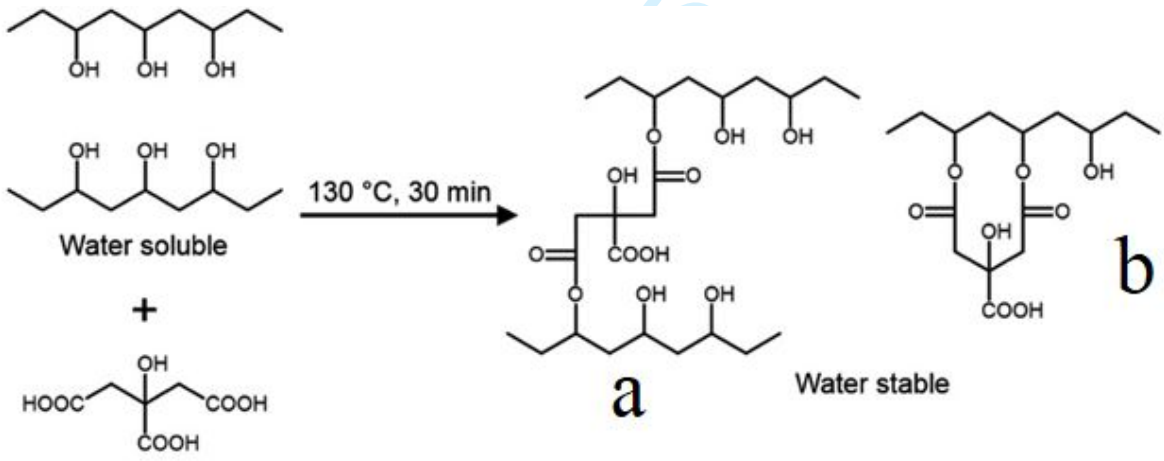
OH
OH
OH
Water soluble
+
HOOC
COOH
COOH
130 °C, 30 min
O
COOH
a
Water stable
b

Fig. 10.

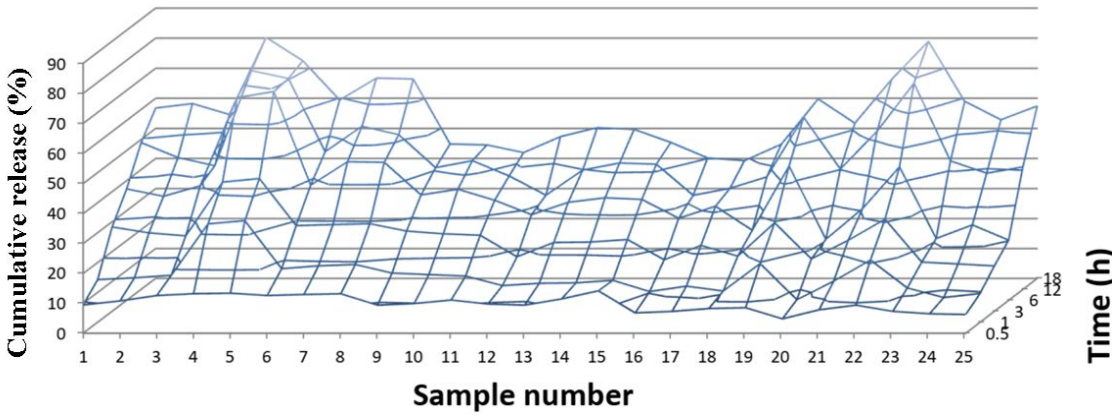
Cumulative release (%)
90
80
70
60
50
40
30
20
10
0
1 2 3 4 5 6 7 8 9 10 11 12 13 14 15 16 17 18 19 20 21 22 23 24 25
Sample number
18
12
6
3
1
0.5
Time (h)

Fig. 11.

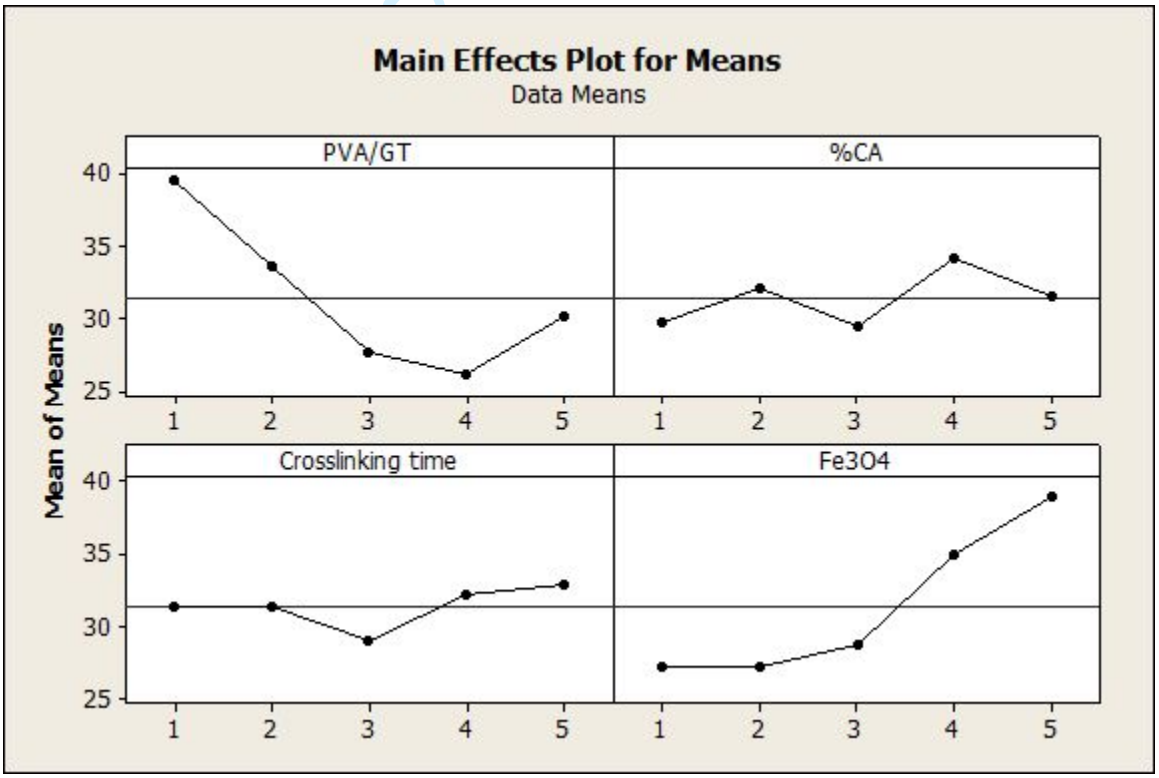
Main Effects Plot for Means
Data Means
PVA/GT
%CA
Crosslinking time
Fe3O4
Mean of Means
40
35
30
25
1 2 3 4 5

Fig. 12.

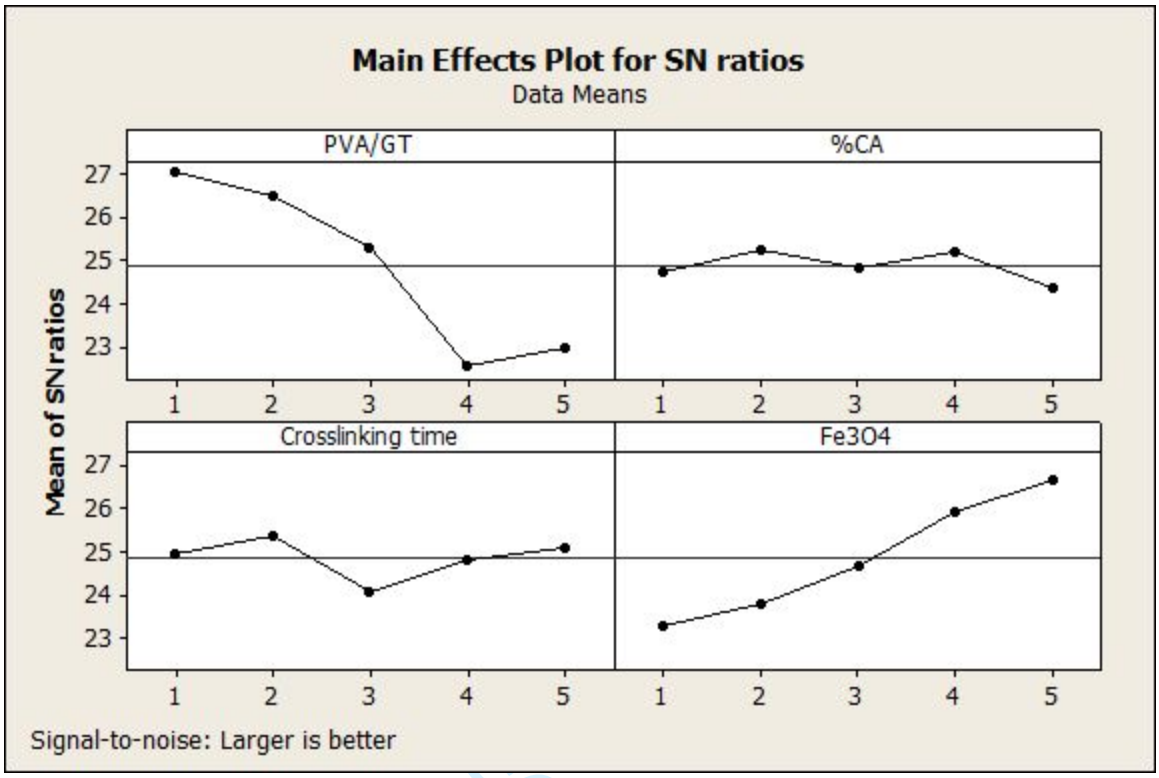
Main Effects Plot for SN ratios
Data Means
PVA/GT
%CA
Crosslinking time
Fe3O4
Mean of SNratios
27
26
25
24
23
1
2
3
4
5
Signal-to-noise: Larger is better

Fig. 13.

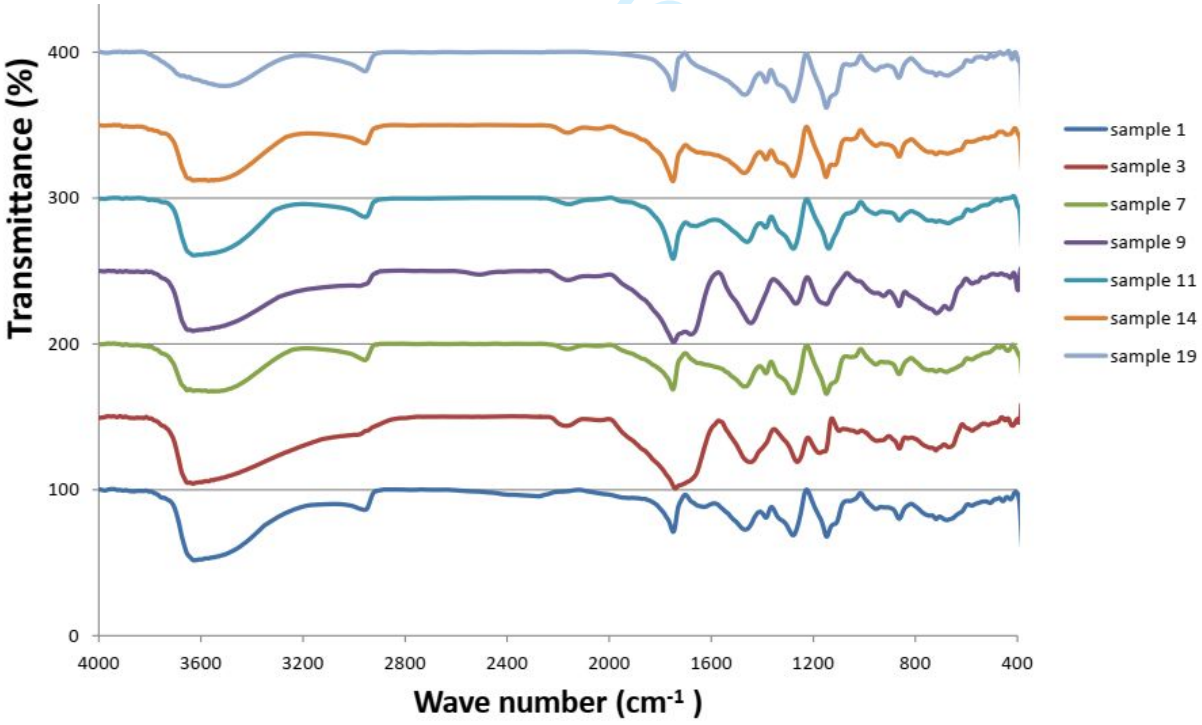
Transmittance (%)
400
300
200
100
0
4000
3600
3200
2800
2400
2000
1600
1200
800
400
Wave number (cm-1)
sample 1
sample 3
sample 7
sample 9
sample 11
sample 14
sample 19

Fig. 14.

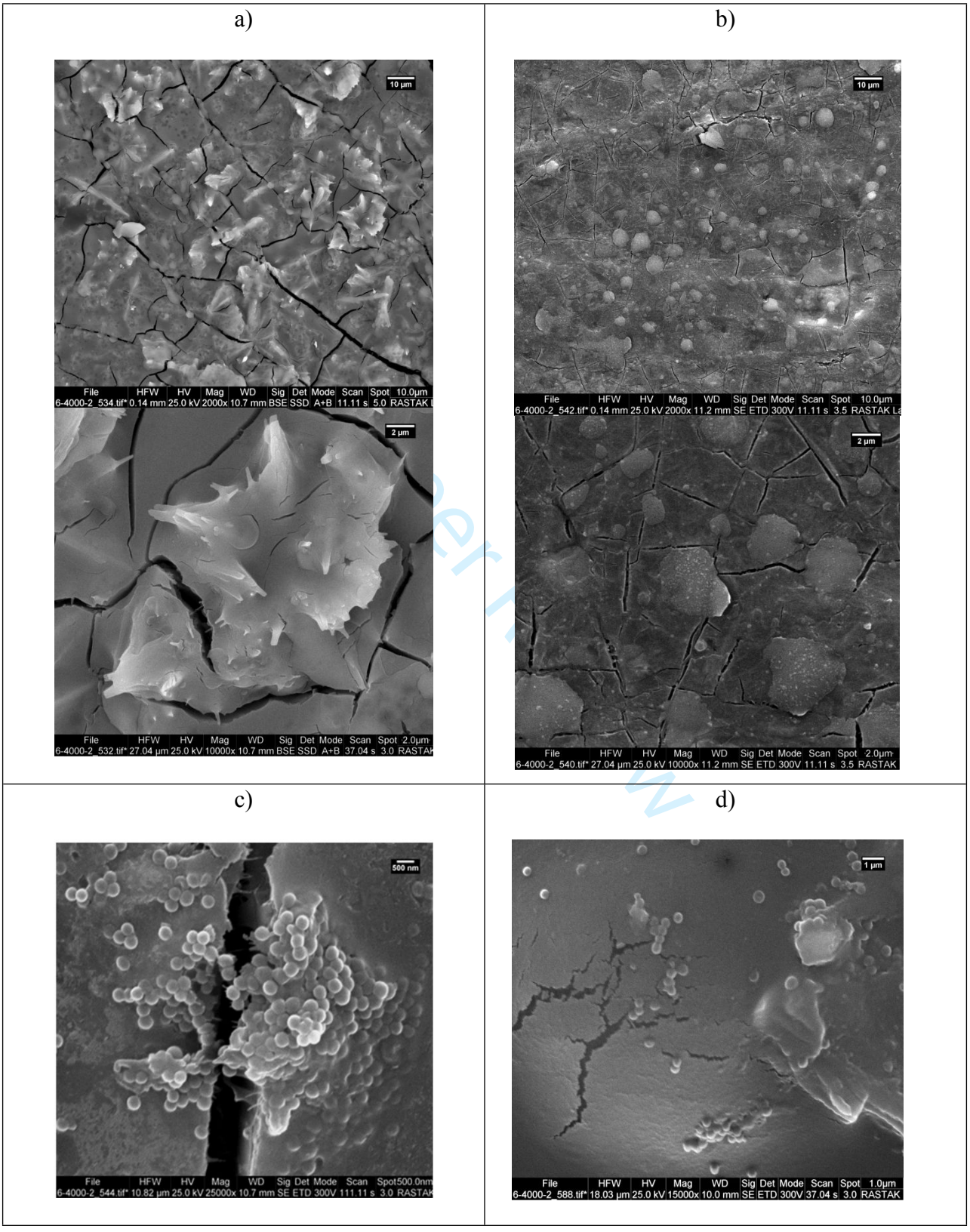

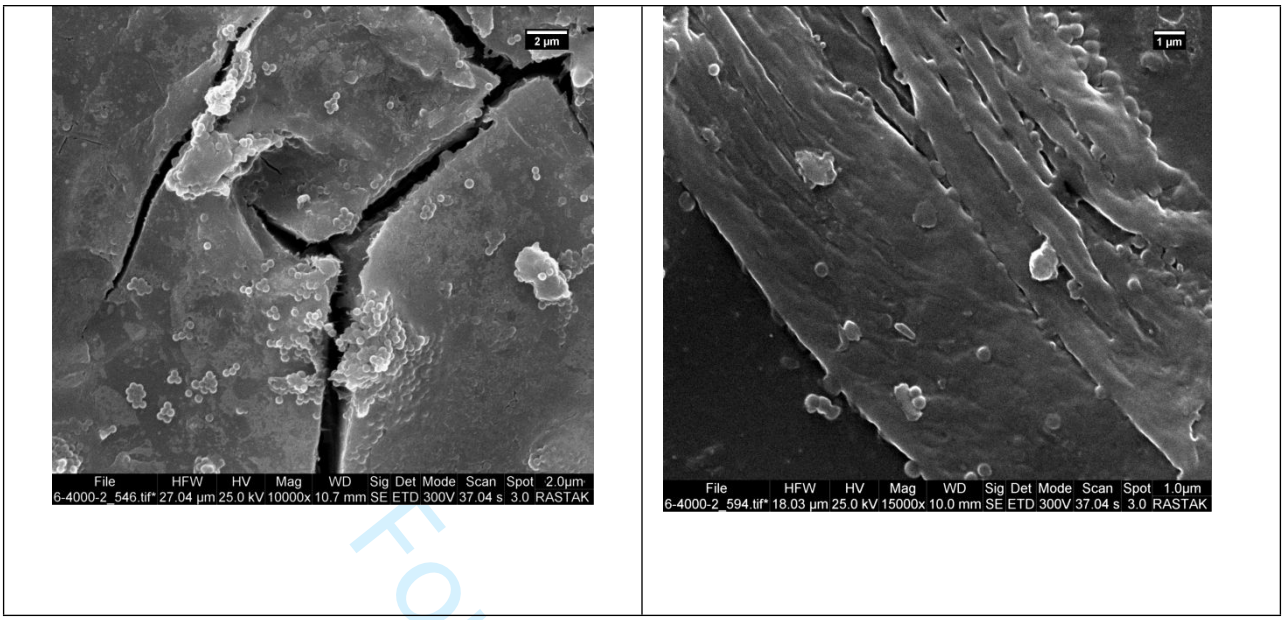

Fig. 15.

Table Captions:
Table 1.

	Levels				
Factors	Level 1	Level 2	Level 3	Level 4	Level 5
PVA/GT(w/w)	1:0	0.95:0.05	0. 9:0.10	0.85:0.15	0.80:0.20
%CA*wt.%	5	4	3	2	1
crosslinking time (min)	1	2	3	4	5
Fe_3O_4*wt.%	1	2	3	4	5

Table 2.

run	PVA (%w/v)	GT (%w/v)	CA*%	Crosslinking Time (min)	Fe_3O_4*%
1	2	0	5	1	1
2	2	0	4	2	2
3	2	0	3	3	3
4	2	0	2	4	4
5	2	0	1	5	5
6	1.9	0.1	5	2	3
7	1.9	0.1	4	3	4
8	1.9	0.1	3	4	5
9	1.9	0.1	2	5	1
10	1.9	0.1	1	1	2
11	1.8	0.2	5	3	5
12	1.8	0.2	4	4	1
13	1.8	0.2	3	5	2
14	1.8	0.2	2	1	3
15	1.8	0.2	1	2	4
16	1.7	0.3	5	4	2
17	1.7	0.3	4	5	3
18	1.7	0.3	3	1	4

19	1.7	0.3	2	2	5
20	1.7	0.3	1	3	1
21	1.6	0.4	5	5	4
22	1.6	0.4	4	1	5
23	1.6	0.4	3	2	1
24	1.6	0.4	2	3	2
25	1.6	0.4	1	4	3

Table 3.

	R^2 results		
run	zero order	Higuchi	Hixon-Crowell
5	0.986	0.933	0.960
25	0.987	0.946	0.962

Table 4.

Carrier	T (^{0}c)	pH	Time	%*Cumulative* Release	refrence
pectin membranes incorporated with cellulose nanocrystals nanofibrils (CNF)	25	6.8	120 min	65%	Zambuzi et al. 2021[31]
copper and aminosilane functionalized mesoporous silica	25	7.2	120 min	58%	Olejnik et al. 2021[32]
biodegradable polymeric sodium alginate and lignosulphonic acid blends	25	7	120 min	72%	Reddy et al. 2021[33]
Fe3O4@SiO2@GLYMO@pectin	37	7.4	120 min	42%	Sadr et al. 2020[9]
Pluronic− HCQ-MTX nanomicelles	37	7.4	5 h	80%	Magne et al. 2021[34]
calcium-alginate beads	37	8	12h	50%	Armutcu et al 2021[35]
Fe_3O_4@GT/PVA hydrogel	25	7.4	18 h	80.28 %	This study